Anomalous temperature and excitation power dependence of cathodoluminescence from InAs quantum dots

Keiichirou Akiba,[1] Naoki Yamamoto,[1,*] Vincenzo Grillo,[2] Akira Genseki,[3] and Yoshio Watanabe[4]
[1]*Department of Physics, Tokyo Institute of Technology, Meguro-ku, Tokyo 152, Japan*
[2]*TASC Institute, INFM, Trieste, Italy*
[3]*Common Research Laboratory, Tokyo Institute of Technology, Meguro-ku, Tokyo 152, Japan*
[4]*NTT Basic Research Laboratories, Atsugi, Kanagawa, 243-0198 Japan*
(Received 6 February 2004; revised manuscript received 2 July 2004; published 28 October 2004)

Self-assembled InAs quantum dots (QDs) in GaAs layers were studied with a cathodoluminescense (CL) detection system combined with a transmission electron microscope. Three distinct peaks were observed to appear in the CL spectrum collected from a $1\mu m^2$ region. The excitation power dependence of the CL spectra and monochromatic CL image observations identified those peaks that are the emissions associated with the ground state and excited state of the QDs in different size groups. Anomalous temperature dependence of those QD emission peaks was observed in the temperature range from 20 to around 100 K, where the emission intensities increase with temperature. Steady-state rate equations for the recombination processes of holes and excitons are proposed with introduction of a potential barrier at the interface between the GaAs layer and the wetting layer (WL). This model can explain the temperature dependence of the emission intensities from the QDs and WL in a wide temperature range.

DOI: 10.1103/PhysRevB.70.165322 PACS number(s): 78.60.Hk, 73.63.Kv, 78.67.Hc

I. INTRODUCTION

Self-assembled InAs quantum dots (QDs) have been intensively studied owing to their potential applications in optoelectronic devices such as lasers,[1] infrared detectors,[2] and optical memory.[3] The three-dimensional (3D) confinement of electrons and holes produces δ-function-like states which provide an important system for fundamental physics and for developing new devices.[4] The InAs strained QDs are spontaneously formed during the epitaxial growth on GaAs in the Stranski-Krastanov (SK) mode, and start to grow as a three-dimensional island on top of a two-dimensional wetting layer (WL). The InAs QDs have inhomogeneity in height and lateral size, which results in a broad luminescence line shape.

In order to realize QD-based optoelectronic devices with high efficiency at room temperature, it is important to understand the temperature dependence of the luminescence intensity from the QD system. Because of the inhomogeneity in QD size, unusual behavior was observed to appear in the temperature dependence and excitation power dependence of the photoluminescence and cathodoluminescence spectra.[5–12] The redshift of the peak energy with increasing temperature is greater than that of the band gap of InAs, and the full width at half maximum (FWHM) of the peak decreases with increasing temperature. This anomaly can be explained by the thermal escape and capture of carriers among the QD states. Thermal quenching of the luminescence from QDs is attributed to the thermal escape of carriers from the QDs to the WL and/or the GaAs barrier layer. However, the coupling among QDs occurs by carrier motion via the WL, and then this makes the diffusion process of the carriers complicated.

Another factor which influences the luminescence line shape is radiative recombination associated with an excited state. An energy relaxation bottleneck is expected for QD,[13] since the energy interval does not match the zone-center LO phonon energy. This causes long lifetime of excitons staying at excited states and increases the emission due to the radiative recombination associated with the excited states of QDs. In the case of quantum wells (QWs), the excitons at the excited state can easily transfer to the ground state by emitting phonons because QW states have band structures. Then the emission intensities associated with excited states are usually very weak in QWs, while in the case of QDs, the emission peaks associated with excited states were frequently observed in photoluminescence and cathodoluminescence (CL) spectra taken under high excitation power.[12,14] This causes a broadening and blueshift of the single broad peak observed in the excitation power dependence for QDs with continuous size distribution.[15] The mode assignment of the excited states has been studied experimentally and theoretically by many authors,[14,16] and recently detailed properties of excited states such as exciton molecules and charged excitons have been found using a single QD measurement.[15,17–19]

Recently we found anomalous temperature dependence of the luminescence intensity in molecular beam epitaxy (MBE) grown InAs QD samples using a cathodoluminescence detection system attached to a transmission electron microscope (TEM). By narrowing the scanning area of the electron beam to a 1 μm region, three distinct emission peaks from the QDs were observed to appear in the CL spectrum. Their emission intensities increased with increasing temperature from 20 K to around 100 K. Then the intensities of the three peaks decrease with further increasing temperature, having maxima at different temperatures. Such anomalous behavior was also observed by other authors with a similar InAs QD contained structure.[20] The excitation power dependence of the CL spectra and the monochromatic CL image observations identified the three peaks that are the emissions associated with the ground state and excited state of the QDs in

different size groups. Their mutual intensities are interchanged with each other as the temperature increases. We propose a steady-state rate equation model for the carrier recombination process. This model can well explain the observed temperature dependence of the luminescence intensities from the QDs as well as that from the WL.

II. EXPERIMENT

Self-assembled InAs quantum dot samples were grown by molecular beam epitaxy (MBE) on Si-doped n^+-type GaAs(001) substrates with a dopant density of 1×10^{18} cm^{-3}.[21] A sample contains three InAs layers with different thicknesses. An InAs layer of 3 monolayer (ML) thickness was deposited on an undoped GaAs buffer layer first grown on the GaAs substrate. Then 2 ML and 1 ML InAs layers were successively deposited with undoped GaAs spacer layers 50 nm thick. Finally, it was capped by a 50 nm GaAs layer on top. The growth rate is 0.33 ML/s for the InAs layers and 1 μm/h for the GaAs spacer layers at 520 °C. The samples were thinned by a Gatan dimple grinder and then Ar ion milling for plan view samples for CL measurement in a transmission electron microscope.

The CL experiments were performed with a modified JEM2000FX TEM at an accelerating voltage of 80 kV with a probe current of 0.9 nA except for the excitation-dependent CL measurement. A probe current ranging from 0.14 to 5.01 nA was used for the excitation-dependent CL measurement. The temperature of the sample was varied from 20 K to 220 K using a liquid He cooling holder. Light from a sample was collected by an ellipsoidal mirror inside the pole piece of an objective lens and focused to the entrance slit of the monochromator. InGaAs/InP photomultiplier tube was used to detect light in the infrared region up to 1700 nm. The system permits spectrally and spatially resolved and polarization-dependent measurements. All the CL spectra shown here were taken with an electron beam scanning over an area of micrometer order (scanning mode) with a probe size of 10 to 20 nm depending on the beam current.

III. RESULTS

Figure 1 reproduces a dark field TEM image of a plan view sample, in which QDs show a diffraction contrast due to the strain fields around them. The density of the QDs is 4×10^{10} cm^{-2}. Their lateral size is distributed in the range from 5 nm to 30 nm in diameter. The histogram of the size distribution shows distinct peaks at diameters of 20 nm and 25 nm. Figure 1 is a projected image along the beam direction, and thus it is difficult to identify the InAs layer to which those QDs belong. TEM observation of a cross section sample showed that the QDs are formed on the 2 ML and 3 ML InAs layers and not on the 1 ML InAs layer.[21] This is plausible because in the SK growth of InAs, a wetting layer 1 ML thick is first formed, and then QDs are generated on it. The majority of them were observed to exist on the 3 ML InAs layer.

Figure 2 shows CL spectra taken at 40 K with electron beam scanning over (a) a 10 μm $\times$ 10 μm area and (b) a 1 μm $\times$ 1 μm area, and (c) with a stationary beam illumination of the same region. In the spectrum from the 10 μm $\times$ 10 μm area, a single broad peak appeared in the energy range from 1.1 eV to 1.35 eV, which is emission from the QDs. The peak appearing at 1.45 eV is emission from the wetting layers. The broad peak has a maximum at 1.2 eV and full width at half maximum of about 100 meV. When the scanning area was narrowed to a 1 μm $\times$ 1 μm area, the single broad peak was split into three sharp peaks at 1.15 eV, 1.20 eV, and 1.25 eV. This suggests that three different groups of QDs are selectively left in this area. The origin of those peaks can be attributed to the size distribution of the QDs and also to emission from excited states in the QDs. To find the origin of each peak we further studied the excitation dependence and temperature dependence of CL spectra, and observed monochromatic CL images using those peak emissions as will be shown in a later section. The CL spectrum was greatly varied by changing the scanning area from place to place, and more complicated spectra involving sharp peaks appeared under the stationary beam illumination condition. However, the three peaks frequently appeared in the CL spectra when taken by scanning over a 1 μm $\times$ 1 μm area. So we took this condition to measure the excitation and temperature dependences. The number of QDs existing in this area is about 400.

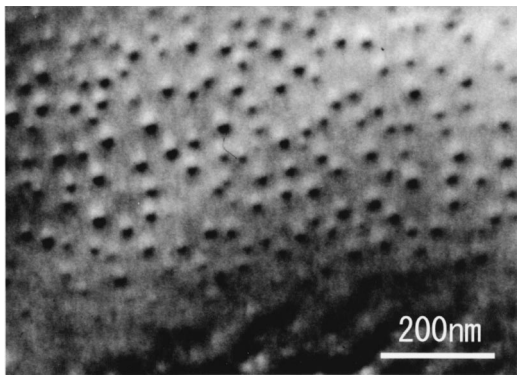

FIG. 1. TEM dark field image of a plan view sample of InAs/GaAs.

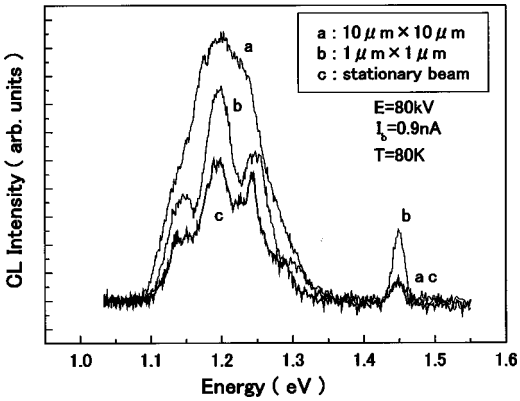

FIG. 2. CL spectra acquired (a) and (b) from scanning areas of (a) 10 μm $\times$ 10 μm and (b) 1 μm $\times$ 1 μm, and (c) with stationary beam illumination. Accelerating voltage is 80 kV, electron beam current 0.9 nA, and a sample temperature 40 K.

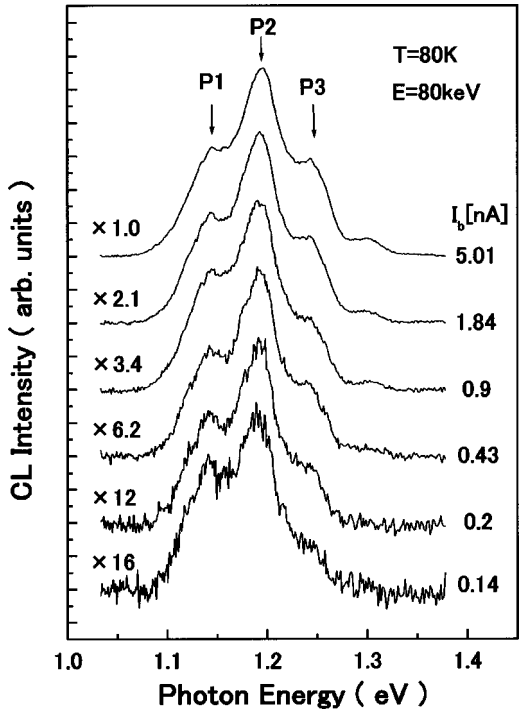

FIG. 3. Excitation power dependence of CL spectra taken for various electron beam currents I_b ranging from 0.14 to 5.01 nA. Accelerating voltage is 80 kV and sample temperature 80 K.

Figure 3 shows CL spectra taken at 80 K for various beam currents I_b ranging from 0.14 to 5.01 nA. There are three peaks appearing in the spectra at peak energies of 1.144 eV (P1), 1.197 eV (P2), and 1.247 eV (P3), respectively. Those peaks have a finite width of about 40 meV, and each of them is composed of emissions from QDs with similar size. Each peak slightly shifts with increasing beam current, by a small blueshift of less than 5 meV. The photon energy of the emission from a single QD is fixed for any excitation rate, because the energy level of the QD is discrete. Therefore an emission peak should not shift, if it comes from a single QD or QDs of fixed size. The slight shift resulting from the increase in excitation rate can be attributed to a change in the population of carriers occupying the QD states of different sizes in each group, which is caused by the reemission and capturing of carriers by the QDs. Another possibility is the appearance of emission from excited states of the larger QDs which happen to have nearly the same energy level as the ground states of the smaller QD groups.

Figure 4 shows the dependence of the CL peak intensity on beam current, which is obtained from Fig. 3. If a luminescence spectrum has a single peak broadened by phonon and impurity scattering, we must take an integrated intensity for the plot. However, in this case the peak is composed of a number of peaks from the QDs with slightly different sizes. The FWHM of each peak is much smaller than the apparent peak width, because it becomes narrower when the illumination area becomes small, as seen in Fig. 2. For this reason we use the peak intensity for the analyses.

The excitation rate dependence of the CL intensity is the same for the P1 and P2 peaks, while the relative increase in intensity is greater for the P3 peak. This fact clearly demonstrates that the P3 emission is due to the transition associated with excited states of the QDs, and thus P1 and P2 emissions should be those associated with the ground states. In most cases the CL intensity varies superlinearly with beam current, i.e., $I_{ph} \propto I_b^k$.[22] The data are fitted with this relation as indicated by the broken lines in Fig. 4. The values of k are 0.74 for P1, 0.78 for P2, and 0.94 for P3, respectively. Then the P3 intensity varies almost linearly with beam current, while the P1 and P2 intensities change more slowly.

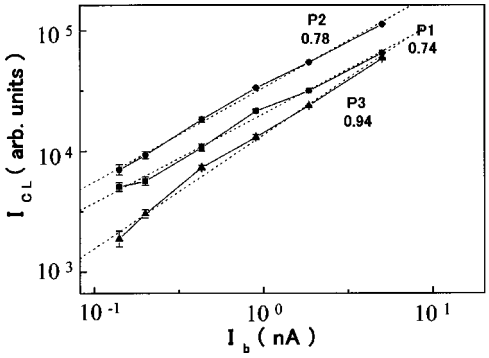

FIG. 4. CL intensities of the P1, P2, and P3 peaks as a function of beam current.

It should be noted that a single broad peak from a wide area (see Fig. 2) shifts to high energies by as much as 50 meV with increasing beam current from 0.2 nA to 10 nA. The relative intensity of the high-energy side increases faster than that of the low-energy side. Then this large blueshift can be understood as an apparent shift due to the appearance of the excited state emission at higher energies.

Figure 5 shows CL spectra taken from the same scanning area as in Fig. 3 at various temperatures ranging from 20 K

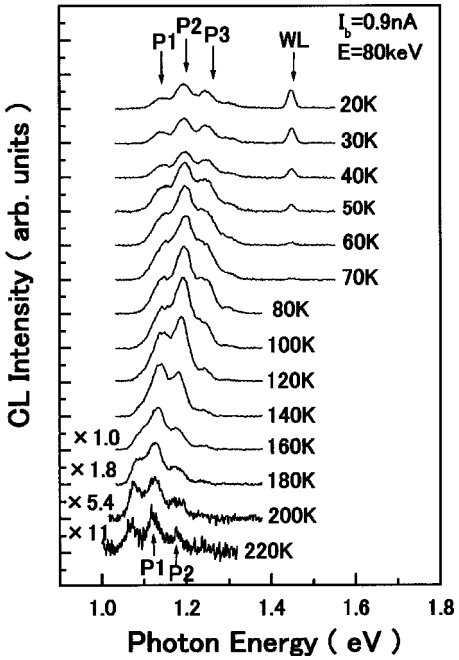

FIG. 5. CL spectra taken at various temperatures ranging from 20 to 220 K. Accelerating voltage is 80 kV and electron beam current is 0.9 nA.

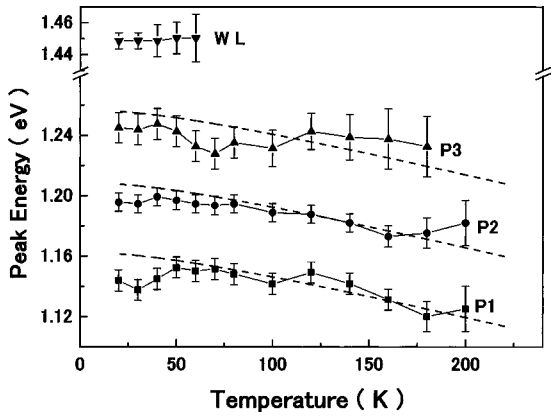

FIG. 6. Photon energies of the P1, P2, P3, and WL peaks vs temperature. The peak energy variations expected from the temperature dependence of the InAs band gap (Varshni's law) are shown by dashed lines.

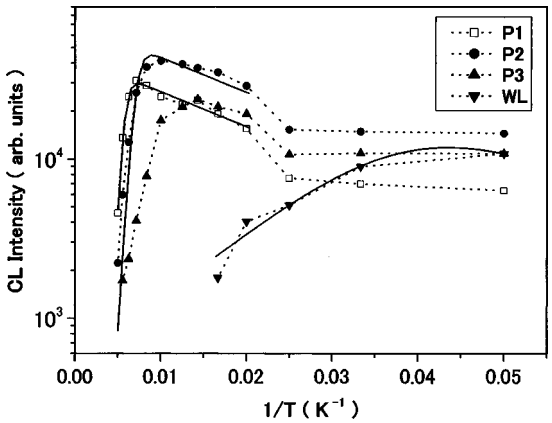

FIG. 7. Arrhenius plot for the CL intensities of the P1, P2, P3, and WL peaks.

to 220 K. The relative intensities of the three peaks (P1, P2, and P3) are seen to change with temperature. At low temperatures high-energy peaks are predominant; the P2 peak is largest at temperatures lower than 120 K. With increasing temperature the P1 peak becomes dominant in the temperature range of 140–180 K. It is noticed that the absolute intensities of those peaks increase as the temperature increases from 20 K to around 100 K, and in turn they decrease for further increase in temperature above 100 K. At the higher temperatures, the high-energy peaks successively decrease and then the lower-energy peaks appear at temperatures above 180 K, which are not resolved from the predominant peaks at low temperatures. A new peak appearing at 1.07 eV is considered to be the luminescence from the other group of QDs with larger size compared to those of the P1 and P2 peaks.

Each peak gradually shifts toward lower energy with increasing temperature. Figure 6 shows the temperature dependence of the observed energies of the three peaks. The dashed lines in Fig. 6 show the expected peak position calculated by using Varshni's law for the band gap variation of InAs using the parameters $\alpha = 0.276$ meV/K and $\beta = 93$ K.[23] The deviation of each peak from the dotted line is small. This ensures that each peak always reflects the luminescence from the same group of QDs at any temperature in this range, and the change in carrier population of the QDs is negligible. In the case of the broad peak emission coming from the QD's with large size distribution, the peak energy greatly deviates from the Varshni law as reported in previous work.[5,8] Such behavior can be understood from the temperature dependence of the relative intensities of the emission peaks seen in Fig. 5.

Figure 7 shows the Arrhenius plot for the P1, P2, P3, and WL peak intensities extracted from the data in Fig. 5. As mentioned before, the P2 peak is dominant at low temperatures below 120 K compared to the P1 and P3 peaks. As temperature increases from 20 K, the intensities of the three peaks are nearly constant up to 40 K, and then they increase from 40 K to around 100 K, while the intensity of the WL peak monotonically decreases and disappears above 60 K. The P3 peak has a maximum at 70 K, and then rapidly decreases with increasing temperature. The P2 and P1 peaks show similar behavior; the P2 and P1 peaks successively have a maximum at 90 K and 140 K, respectively.

The intensity decay at high temperatures from 100 to 200 K is attributed to thermal excitation of carriers from QD states to WL states. Thermal excitation of carriers from the QDs to the GaAs band was reported to occur at further high temperatures above 200 K,[12] though sufficient data could not be obtained in the present study because of the small intensities in this temperature range. From the slope of the Arrhenius plot, the activation energies are derived to be 170 meV (E_1), 125 meV (E_2), and 44 meV (E_3) for the P1, P2, and P3 peaks, respectively. Those energies correspond to the binding energy for carriers escaping from the depth of energy levels in the QDs with respect to that of the WL. The carriers in those levels can escape from the QDs when the thermal energy becomes comparable to the binding energy. Therefore this can well explain the shape of the curves in the high-temperature region in Fig. 7. The binding energy from the QD state to the WL state is smaller for the smaller QDs which give the higher-energy peak emission. Then the rapid decrease starts at the lower temperature for the higher-energy peak, i.e., the P2 peak intensity has a maximum at a lower temperature than that of the P1 peak.

The decrease in CL intensity at low temperatures below 80 K is unusual, and we must consider another mechanism for carrier diffusion and recombination processes. We propose a model in the next session.

Figure 8 shows the monochromatic CL images taken at various photon energies. This measurement was performed at 40 K for the scanning area of 10 μm $\times$ 10 μm including the same area used for the excitation and temperature dependence measurements (Figs. 3 and 5). Figures 8(a)–8(f) are monochromatic CL images taken at photon energies of the (a) P1 peak, (b) P2 peak, (c) P3 peak, and (d) WL peak, respectively. The intensity distribution in each CL image indicates the spatial distribution of the QDs in the same group of similar size. The CL intensity distributions of the P1–P3 emission have rather similar shapes to each other, while the intensity distribution of the WL emission is complementary to those. This does not mean that the WL is not uniform. The

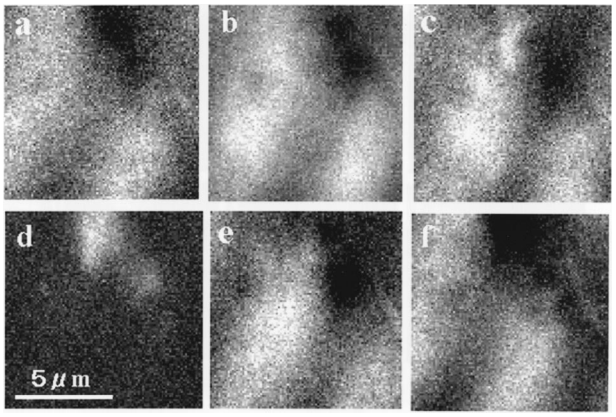

FIG. 8. Monochromatic CL images of the InAs/GaAs thin sample taken at 40 K using photon energies of (a) 1.144 eV (P1), (b) 1.197 eV (P2), (c) 1.247 eV (P3), (d) 1.449 eV (WL), (e) 1.181 eV, and (f) 1.211 eV. The scan area is 10 μm$\times$10 μm.

origin of the contrast could be an inhomogeneous distribution of QDs, and the WL emission increases in the low-density region of QDs, because the two emissions are competitive in the carrier recombination process. The P3 emission is associated with the excitation state as mentioned before, and the CL image [Fig. 8(c)] is obviously different from that of P1 [Fig. 8(a)], but is similar to that of P2 [Fig. 8(b)]. For more precise comparison, we observed monochromatic CL images at slightly lower (1.181 eV) and higher (1.211 eV) energies from the P2 peak (1.197 eV), which are shown in Figs. 8(e) and 8(f), respectively. The intensity distribution in Fig. 8(e) closely resembles that of P3. This indicates that the emission energy from the ground state related to the excited state of P3 is close to but slightly lower than the P2 peak energy. Thus, the energy difference between the ground and the excited states is about 70 meV. In addition the intensity distribution in Fig. 8(f) is quite similar to that of P1 [Fig. 8(a)]. This means that the emission from the excited state related to the P1 ground state appears near the P2 peak in the CL spectrum with an energy difference of about 70 meV.

From these results we can identify the recombination associated with the P1 to P3 emissions as schematically depicted in Fig. 9. The P1 emission is associated with the ground state in the larger QDs, and the P2 and P3 emissions are associated with the ground and excited states in the smaller QDs. The energy level significantly depends on the height of the QD, but not on the lateral dimension, because the height is much smaller than the lateral dimension in these QDs. However, a close relation between the height and lateral dimension of a QD can be expected. The large and small QDs are mixed in the InAs layers, as found from the observation where the CL intensity distributions of the P1 and P2 emissions are spatially overlapped in the CL images. One simple explanation for the existence of different size groups is that they are formed in the 2 and 3 ML InAs layers separately. However, a cross sectional TEM image showed that both larger and smaller QDs are equally formed in the 3 ML InAs layer. Such a size distribution has also been observed by other authors.[24]

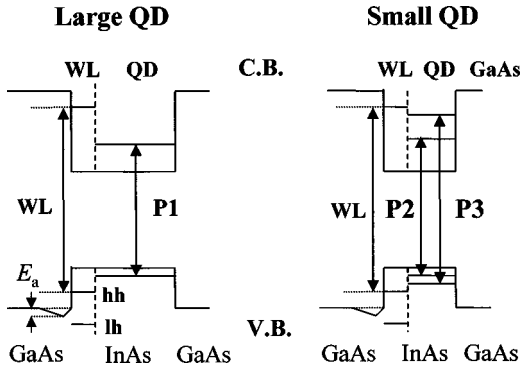

FIG. 9. Energy diagrams of the InAs QDs–GaAs system for the QD groups with large and small sizes. A potential barrier of energy E_a for heavy holes (HH) is formed at the interface between the GaAs layer and the WL.

IV. DISCUSSION

An anomalous temperature dependence of the CL emission intensities from QDs of different sizes was observed as shown in Fig. 5 and Fig. 7. The carrier dynamics can be derived by analyzing those behaviors of the emission intensities, though the system is rather complicated because of the existence of the WL. In this section we mainly deal with rate equations for the carrier recombination processes in this system and explain the anomalous behavior.

First we consider the generation process of carriers by the incident electron beam and their diffusion process in the sample. Incident electrons are elastically scattered in a thin sample and generate electron-hole pairs along the trajectory of the electrons through the successive excitations of secondary electrons and plasmons.[25] The generation volume of the carriers is nearly a cone shape expanding toward the bottom of the thin sample. The thickness of the observed area is about 700 nm, and the InAs layers are located within a thickness of 150 nm from the top surface. Then a major part of the carriers is generated in the lower undoped GaAs region below the InAs layers. After generation, those carriers migrate to the surrounding region by diffusion. The diffusion length in undoped GaAs is reported to be 0.69 μm for electrons at room temperature.[26] Therefore major parts of the electrons can reach the WL of the 3 ML InAs layer, or recombine nonradiatively at the bottom surface without recombining in the GaAs region. This is consistent with the observation that there is no CL emission from the GaAs layer even at low temperatures. The diffusion length for holes is much smaller than that for electrons, and thus the number of holes reaching the WL is not as great as that of electrons. The carriers captured by the WL tend to form excitons, though they are thermally dissociated into single carriers at high temperatures. These carriers move around in the WL and are trapped by QDs to emit light without nonradiative recombination. Thus the observed QD emission is mainly generated in the QDs in the 3 ML InAs layer. As the temperature increases, the reemission of carriers from the QDs to the WL and the WL to GaAs becomes dominant, which changes the relative emission intensities of the QDs and WL.

A diagram for the carrier flow process is schematically represented in Fig. 10. In the diagram, G stands for the gen-

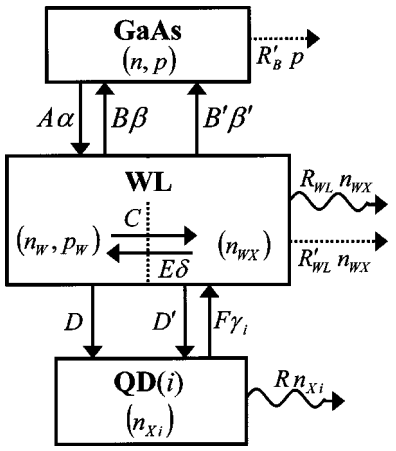

FIG. 10. Schematic of the rate equation model. Carrier density is indicated by n and p for electrons and holes in GaAs, respectively, and n_w and p_w in the WL. Exciton density is indicated by n_{WX} in the WL and $n_{X\,i}$ in the i-th QD.

eration rate of electron-hole pairs, which is proportional to the incident electron beam current I_b. The hole density is smaller than that of electrons in the GaAs and WL in the steady state, because the lifetime of the holes is shorter. Therefore the holes are regarded as a minority carrier in this system. Thus we deal only with the behavior of the holes in the rate equations. The hole densities in the GaAs layer and WL are represented by p and p_W, respectively, and electron densities in the WL by n_W. The exciton densities in the WL and ith QD ($i=1,2$) are, represented by n_{WX} and n_{Xi}, respectively. Radiative and nonradiative, recombination rates are expressed as R and R' with subscription of each region. The rate equations for holes and excitons in each region are written as follows:

$$\frac{dp}{dt} = G - A\alpha p - R'_B p + B\beta p_W + B'\beta' n_{WX}, \tag{1}$$

$$\frac{dp_W}{dt} = A\alpha p - B\beta p_W - Cn_W p_W - D\sum_i p_W(N_i - n_{Xi}) + E\delta n_{WX}, \tag{2}$$

$$\frac{dn_{WX}}{dt} = Cn_W p_W - (R_W + R'_W)n_{WX} - B'\beta' n_{WX} - D'\sum_i n_{WX}(N_i - n_{Xi}) - E\delta n_{WX} + F\sum_i n_{Xi}\gamma_i, \tag{3}$$

$$\frac{dn_{Xi}}{dt} = Dp_W(N_i - n_{Xi}) + D'n_{WX}(N_i - n_{Xi}) - F\gamma_i n_{Xi} - Rn_{Xi}, \tag{4}$$

where

$$\alpha = \exp\left(-\frac{E_a}{kT}\right), \quad \beta = \exp\left(-\frac{E_B^h - E_{WL}^h}{kT}\right),$$

$$\beta' = \exp\left(-\frac{E_{BW}}{kT}\right).$$

$$\gamma_i = \exp\left(-\frac{E_i}{kT}\right), \quad \delta = \exp\left(-\frac{E_{XW}}{kT}\right) \tag{5}$$

Here we adopt similar assumptions proposed by Sanguinetti *et al.*[11] The terms involving factors β and β' express the reemission of holes and excitons from the WL to GaAs layer, and that involving γ_i expresses reemission of excitons from the ith QD to the WL. The term $Cn_W p_W$ indicates the generation rate of excitons in the WL, and $E\delta n_W$ indicates dissociation rate of excitons into single carriers. For simplicity it is assumed that the QDs are electrically neutral, and then the electrons and holes captured by the QDs instantaneously form excitons. The reemission of electrons and holes from the QD to WL is assumed to occur in a correlated manner[27] as well as that from the WL to GaAs.[28] We also consider only two sizes of QDs corresponding to the peak emissions P1 and P2, and ignore the size distribution of QDs.

We introduce two important ideas in the proposed model. One is seen in Eq. (1), which is the rate equation for holes in the undoped GaAs layer. The second term $A\alpha\, p$ shows a capture rate of holes by the WL, where we introduce a temperature-dependent factor α, which involves an activation energy E_a. This energy expresses a small potential barrier for holes captured by the WL from the GaAs layer as schematically depicted in Fig. 9. This potential barrier acts as an obstacle for the holes flowing from the GaAs layer into the WL, which can be the origin of the increase in QD emission with increasing temperature. The second idea is that the contribution of single carriers is explicitly involved in the rate equation for the WL, i.e., the terms involving p_W in Eq. (2), which has been ignored in previous theories,[11,20] because the exciton term is considered to be more dominant. However, the single-carrier terms become important in explaining the behavior of the QD and WL emissions at wide temperature range. Next we will derive the temperature dependences of emission intensities from the QDs and WL by using this model for two temperature regimes.

At low temperatures below 60 K, the WL emission has strong intensity comparable with those of the QD emissions. In Fig. 7 the WL emission decreases with increasing temperature, and becomes negligibly small at 80 K. The same behavior should occur for the exciton density in the WL, n_{WX}, because it is proportional to the WL emission intensity. In this temperature range, it is plausible to consider that $n_{WX} \gg p_W$ and $\gamma_i \cong 0$. In the steady state, the above rate equations are reduced to

$$G - A\alpha p - R'_B p + B\beta p_W + B'\beta' n_{WX} = 0, \tag{6}$$

$$A\alpha p - Cn_W p_W - DNp_W + E\delta n_{WX} = 0, \tag{7}$$

$$Cn_W p_W - (R_W + R'_W)n_{WX} - B'\beta' n_{WX} - D'Nn_{WX} - E\delta n_{WX} = 0, \tag{8}$$

$$DNp_W + D'Nn_{WX} - Rn_{Xi} = 0. \tag{9}$$

Here we assume that the QDs are far from saturation, and then $\Sigma_i N_i - n_{Xi} \cong \Sigma_i N_i = N$, where N is the total number of QDs concerned here. In Eq. (6) the last two terms are small compared to the others and can be neglected. Then we obtain

$$p = \frac{1}{A\alpha + R'_B} G. \tag{10}$$

At low temperatures, it is expected that the electrons and holes in the WL tend to trap each other to produce excitons before captured by QDs. Then neglecting the last two terms in Eq. (7), we get

$$A\alpha p - Cn_W p_W \cong 0. \tag{11}$$

Using Eqs.(10) and (11), the exciton density in the WL can be obtained from Eq. (8) as

$$n_{WX} = (D'N + R_W + R'_W + B'\beta + E\delta)^{-1}\left(1 + \frac{R'_B}{A}\alpha^{-1}\right)^{-1} G. \tag{12}$$

The emission intensity of excitons in the WL is given by

$$I_W = R_W n_{WX}. \tag{13}$$

The expression in the second parentheses in Eq. (12) is nearly constant at low temperatures, and thus the temperature-dependence of the WL emission comes from the expression in the first parentheses involving the two temperature-dependent terms. We can deduce the activation energy in β or δ by fitting with the observed curve in Fig. 7. The solid line in Fig. 7 is a calculated curve for the WL emission, fitted with a simple formula involving a single temperature dependent factor in the first parentheses in Eq. (12), using the parameters in the second parentheses obtained from the fitting of I_i at higher temperatures as shown later. From this fitting the activation energy is obtained to be 13 meV. The binding energy E_{XW} of the exciton in the WL was recently calculated to be 12.9 meV for a 1 ML InAs quantum well in GaAs on the basis of the tight-binding approach;[29] while the activation energy E_{BW} for excitons or electron-hole pairs thermally emitted from the quantum well to the barrier is considered to be half of the total confinement energy of the electon-hole pair in the quantum well.[28] In the present case $E_{BW} = (1/2)(E_{\mathrm{GaAs}} - E_{WL}) = 29$ meV with $E_{\mathrm{GaAs}} = 1.507$ eV and $E_{WL} = 1.449$ eV at 80 K. Thus the activation energy obtained from the fitting is close to the exciton binding energy E_{XW}. This means that the decrease in the WL emission around 60 K is caused by the dissociation process of excitons in the WL.

On the other hand, from Eq. (9), we obtain the emission intensity from the ith QD as

$$I_i = Rn_{Xi} = DN_i p_W + D'N_i n_{WX}. \tag{14}$$

If the first term associated with the capture rate of holes by QDs is ignored, the QD emission intensity is proportional to n_{WX} or I_W. This approximation can be valid in the very low-temperature range below 30 K, but not in the temperature range above 30 K where I_i is nearly constant or rather increasing with increasing temperature in contrast to the decrease of I_W. Therefore a model which treats only the behavior of excitons cannot explain the temperature dependences of the QD and WL emissions at the same time. This is the reason why we leave the terms associated with holes in the rate equations.

In the higher temperature range from 50 to 220 K, we may approximate that $n_{WX} \cong 0$, and $DNp_W \gg Cn_W p_W$. Then the rate equation is reduced to

$$G - A\alpha p - R'_B p + B\beta p_W = 0, \tag{15}$$

$$A\alpha p - B\beta p_W - DNp_W = 0, \tag{16}$$

$$Dp_W N_i - E\gamma_i n_{Xi} - Rn_{Xi} = 0. \tag{17}$$

In Eq. (15) the last term is still smaller than the other terms, and then Eq. (10) for p holds. From Eqs. (16) and (17) we get

$$p_W = \frac{A\alpha}{B\beta + DN} p \cong \frac{A\alpha}{DN} p, \tag{18}$$

$$n_{Xi} = \frac{DN_i}{R + E\gamma_i} p_W. \tag{19}$$

Then the emission intensity from the ith QDs is expressed as

$$I_i = R\, n_i = \frac{N_i}{N}\left(1 + \frac{E}{R}\gamma_i\right)^{-1}\left(1 + \frac{R'_B}{A}\alpha^{-1}\right)^{-1} G. \tag{20}$$

The solid curves fitted to the P1 and P2 emissions in Fig. 7 are calculated using Eq. (20). The expression in the first parentheses expresses the quenching of the QD emissions in the high-temperature range from 100 to 220 K, while the expression in the second parentheses gives the increase in the QD emissions with increasing temperature from 50 to around 100 K. The fitting parameters are as follows: $E_1 = 216$ meV, $E_2 = 175$ meV, and $E_a = 4.4$ meV. The ratio N_1/N_2 is also determined from the fittings to be 1.60. The fitting curves well reproduce the observed ones using common parameters of E_a, E/R, and R'_B/A. The values of E_1 and E_2 are slightly larger than those obtained from the linear slope measurements in Fig. 7.

The appearance of the potential barrier E_a can be attributed to band bending due to the strain field induced by the lattice misfit between the GaAs and InAs layers. The lattice misfit in the (001) plane, $(a_{\mathrm{InAs}} - a_{\mathrm{GaAs}})/a_{\mathrm{GaAs}}$, is 7.17×10^{-2}. A large amount of it can be relaxed in the InAs layer, but the rest of it causes a biaxial tensile strain in the GaAs layer near the interface. Using the deformation potentials and elastic constants, the valence band edge sifts induced by a strain ε are expressed by[30]

$$\delta E_\nu = -2a_\nu\left(1 - \frac{C_{12}}{C_{11}}\right)\varepsilon \pm 2b\left(1 + 2\frac{C_{12}}{C_{11}}\right)\varepsilon,$$

where the plus and minus signs are for the heavy hole (HH)

and light hole (LH), respectively. For GaAs with $a_v = -1.00$ eV, $b = -1.8$ eV, $C_{11} = 832.9$ GPa, and $C_{12} = 452.6$ GPa, we get $\delta E_v = 8.43\varepsilon$ eV for the HH, and $\delta E_v = -6.60\varepsilon$ eV for the LH.[23] This means that the band gap for the HH in the GaAs layer increases near the interface, while for the LH it decreases. For an HH the valence band edge of the InAs WL is lower than that of GaAs, while for a LH the valence band edge of the WL is higher than that of GaAs. Then the holes are in the HH state in the WL, and combine with the conduction band electrons to form excitons or are captured by the QDs to become HH excitons in the QDs. Therefore we should consider the flow process of the HH from the GaAs layer rather than that of the LH. Jiang *et al.*[20] consider the transition process for the LH exciton to transfer into QDs through LH states in the WL. However, this process cannot be dominant because the transition probability of holes and excitons to the LH state in the WL should be much smaller than that to the HH state. Thus it is unlikely that this process is the origin of the anomalous temperature dependence. The energy barrier derived from the fitting is 4.4 meV. If this corresponds to the valence band shift of the HH, the biaxial strain is estimated to be 5.2×10^{-4} using the above equation. This value is two orders of magnitude smaller than the lattice misfit between GaAs and InAs in the (001) plane. It is plausible that such a small strain is left in the GaAs layer near the interface.

V. CONCLUSION

Self-assembled InAs quantum dots in GaAs layers were studied by a cathodoluminescece detection system combined with TEM. Three distinct peaks are observed to appear in the CL spectrum by narrowing the beam scanning area to a 1 μm^2 region. The excitation rate dependence of the CL spectra and the monochromatic CL image observations identified those peaks: the lowest-energy peak (P1) is the emission associated with the ground state of the large size QDs, and the higher-energy peaks (P2 and P3) are the emissions associated with the ground state and excited state of the small sized QDs, respectively. As the temperature increases from 20 K, the emission intensities of those QD peaks first increase as much as three times from 20 to around 100 K, while that of the WL peak decreases and disappears above 60 K. This anomalous temperature dependence of the QD emission peaks was simulated using the rate equations for carriers in the steady state. In the model we proposed the existence of a potential barrier at the interface between the GaAs layer and the WL. The barrier height is derived from the fitting to be about 4 meV, which can be attributed to the band shift due to the strain field generated by the lattice mismatch between the two layers. We also deal with the rate equation for holes as well as excitons, and can consistently explain the temperature dependence of the emission intensities from the QDs and the WL.

*Corresponding author. Electronic address: nyamamot@surface.phys.titech.ac.jp

[1] N. N. Ledentsov, M. Grundmann, N. Kirstaedter, O. Schmidt, R. Heitz, J. Böhrer, D. Bimberg, V. M. Ustinov, V. A. Shchukin, A. Yu. Egorov, A. E. Zhukov, S. Zaitsev, P. S. Kop'ev, Zh. I. Alferov, S. S. Ruvimov, A. O. Kosogov, P. Werner, U. Gösele, and J. Heydenreich, Solid-State Electron. **40**, 785 (1996).
[2] K. W. Berryman, S. A. Lyon, and M. Segev, Appl. Phys. Lett. **70**, 1861 (1997).
[3] K. Tamamura, Y. Sugiyama, Y. Nakata, S. Muto, and N. Yokoyama, Jpn. J. Appl. Phys., Part 2 **34**, L1445 (1995).
[4] D. Bimberg, M. Grundmann, and N. N. Ledentsov, *Quantum Dot Heterostructures* (Wiley, New York, 1998).
[5] L. Brusaferri, S. Sangunetti, E. Grilli, M. Guzzi, A. Bignazzi, F. Bogani, L. Carraresi, M. Colocci, A. Bosacchi, P. Frigeri, and S. Franchi, Appl. Phys. Lett. **69**, 3354 (1996).
[6] D. I. Lubyshev, P. P. González-Borrero, E. Marega, Jr., E. Petitprez, N. La Scala, Jr., and P. Basmaji, Appl. Phys. Lett. **68**, 205 (1996).
[7] H. Lee, W. Yang, and P. C. Sercel, Phys. Rev. B **55**, 9757 (1997).
[8] Z. Y. Xu, Z. D. Lu, X. P. Yang, Z. L. Yuan, B. Z. Zheng, J. Z. Xu, W. K. Ge, Y. Wang, J. Wang, and L. L. Chang, Phys. Rev. B **54**, 11 528 (1996).
[9] S. Farard, S. Raymond, G. Wang, R. Leon, D. Leonard, S. Charbonneau, J. L. Merz, P. M. Petroff, and J. E. Browers, Surf. Sci. **361/362**, 778 (1996).
[10] W. Yang, R. R. Lowe-Webb, H. Lee, and P. C. Sercel, Phys. Rev. B **56**, 13 314 (1997).
[11] S. Sanguinetti, M. Henini, M. Grassi Alessi, M. Capizzi, P. Frigeri, and S. Franchi, Phys. Rev. B **60**, 8276 (1999).
[12] Y. Tang, D. H. Rich, I. Mukhametzhanov, P. Chen, and Madhukar, J. Appl. Phys. **84**, 3342 (1998).
[13] H. Bebisty, Phys. Rev. B **51**, 13 281 (1995).
[14] M. Grundmann *et al.*, Appl. Phys. Lett. **68**, 979 (1996).
[15] I. Strichmann, C. Metzner, B. D. Gerardot, W. N. Schoenfeld, and P. M. Petroff, Phys. Rev. B **65**, 081303(R) (2002).
[16] S. Noda, T. Abe, and M. Tamura, Phys. Rev. B **58**, 7181 (1998).
[17] M. Bier, F. Findeis, A. Zrenner, M. Bichler, and G. Abstreiter, Phys. Rev. B **64**, 195326 (2001).
[18] E. Dekel, D. Gershonj, E. Ehrenfreund, J. M. Garcia, and P. M. Petroff, Phys. Rev. B **61**, 11 009 (2000).
[19] D. V. Regelmann, D. Gershoni, E. Ehrenfreund, W. N. Schoenfeld, and P. M. Petroff, Physica E (Amsterdam) **13**, 114 (2002).
[20] W. H. Jiang, X. L. Ye, B. Xu, H. Z. Xu, D. Ding, J. B. Liang, and Z. G. Wang, J. Appl. Phys. **88**, 2529 (2000).
[21] V. Grillo, A. Genseki, N. Yamamoto, and Y. Watanabe, Surf. Interface Anal. **35**, 40 (2003).
[22] T. Schmidt, K. Lischka, and W. Zulehner, Phys. Rev. B **45**, 8989 (1992).
[23] I. Vurgaftman, J. R. Meyer, and L. R. Ram-Mohan, J. Appl. Phys. **89**, 5815 (2001).
[24] C. A. Duarte, E. C. F. da Silva, A. A. Quivy, M. J. da Silva, S. Martini, J. R. Leite, E. A. Meneses, and E. Lauretto, J. Appl. Phys. **93**, 6279 (2003).
[25] H. E. Bishop, in *Quantitative Scanning Electron Microscopy*, edited byD. B. Holt, M. D. Muir, P. R. Grant, and I. M. Boswarva,

(Academic, New York, 1974), p. 41
[26] H. A. Zarem, P. C. Sercel, J. A. Lebens, L. E. Eng, A. Yariv, and K. J. Vahala, Appl. Phys. Lett. **55**, 1647 (1989).
[27] W. Yang, R. R. Lowe-Webb, H. Lee, and P. Sercel, Phys. Rev. B **56**, 13 314 (1997).
[28] P. Michler, A. Hangleiter, M. Moser, M. Geiger, and F. Scholz, Phys. Rev. B **46**, 7280 (1992).
[29] R. C. Iotti and L. C. Andreani, Phys. Rev. B **57**, R15 072 (1998).
[30] S. L. Chuang, Phys. Rev. B **43**, 9649 (1991).